

Corrosion Protection of Copper in 3% NaCl Solution by the Fabrication of Thiadiazole Monolayer

P. Durainatarajan¹, M. Prabakaran², S. Ramesh^{1,*}, and V. Periasamy¹

¹Department of Chemistry, The Gandhigram Rural Institute-Deemed University, Gandhigram 624302, Tamil Nadu, India

²Department of Chemistry, Gnanamani College of Technology, Namakkal 637018, Tamil Nadu, India

In this study, 2-mercapto-1,3,4-thiadiazole (2-MT) self-assembled monolayer (SAM) was formed on copper electrode surface and the resulting 2-MT SAM on copper has been characterized using surface analytical techniques such as Fourier transform infrared (FT-IR) spectroscopy, energy dispersive X-ray (EDX) analysis, atomic force microscopy (AFM) and contact angle measurement (CA). The existence of N and S in the EDX and FT-IR analysis showed that 2-MT molecules were self-assembled on the copper through N and S by chemisorption which indicates the formation of 2-MT SAM on copper surface. Corrosion protection performance of 2-MT SAM on copper was investigated using potentiodynamic polarization studies (PDS), cyclic voltammetry (CV) and scanning electron microscopy (SEM), respectively. Analysis of both electrochemical and SEM analysis results revealed excellent corrosion protection for the copper substrate.

Keywords: Corrosion, Self-Assembled Monolayer, Atomic Force Microscopy.

1. INTRODUCTION

Copper is one of the most prime metals which has been widely used in circuit components, circuit board, architecture, automotive, power transmission line, seawater systems and industrial sector etc. due to its good thermal and electrical conductivities.^{1,2} However, in the chloride-containing aqueous environment, the copper materials have been susceptible to corrosion and this affects its industrial applications, economy and society.³⁻⁵ In order to reduce or minimize the metallic corrosion, many corrosion control strategies have been employed, namely corrosion inhibitors, cathodic protection and self-assembly technique. Among these methods, surface modifications of metal with self-assembled monolayer (SAM) acts as robust barrier to protect copper against corrosion.^{6,7} The SAM technique has attracted much attention in the coating and corrosion prevention due to ease of assembly, manipulation and characterization.⁸ Generally, heterocyclic organic compounds comprising nitrogen and sulfur atom as well as conjugated pi bonds in their molecular structures are found to be excellent corrosion inhibitors for many metals and alloys in various chloride media.⁹⁻¹⁸ On the other hand, the environmental toxicity of heterocyclic organic

inhibitor molecules limits their application in industries. Therefore, thiadiazole and its derivatives are well known due to their non-toxicity and good corrosion inhibitor in different media.^{11, 19-21}

In the present study, 2-mercapto-1,3,4-thiadiazole (Fig. 1) inhibitor was employed as a corrosion inhibitor against copper corrosion. It consists of nitrogen and sulfur containing five member ring and mercapto group which are the potential binding sites and they can interact with metals to form a compact protective film on the substrate. Very few studies have been performed on corrosion protection of copper by self-assembly of nitrogen and sulphur bearing heterocyclic molecules.²²⁻²⁴ In this context, we attempt to form 2-mercapto-1,3,4-thiadiazole on electrode surface and to assess its corrosion protection properties for copper in NaCl solution.

2. EXPERIMENTAL DETAILS

2.1. Materials and Electrode Preparation

All the chemical components used in this experiment are as follows: 2-mercapto-1,3,4-thiadiazole (2-MT, Alfa aesar, 98%) sodium chloride (NaCl, Merck, 99%) and anhydrous ethanol (CH₃CH₂OH) were of analytical reagent (AR) grade and were used as received. The 2-MT compound was dissolved in anhydrous ethanol

*Author to whom correspondence should be addressed.

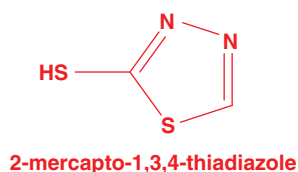


Figure 1. Chemical structure of 2-mercapto-1,3,4-thiadiazole.

to prepare the different assembling solutions (0.1, 0.5, 1.0 and 1.5 mM). For the electrochemical investigation, the working copper electrode was abraded with different grades of emery papers (1/0 up to 6/0) and then decreased with alumina slurries (0.3 μm) and consecutively washed with double distilled water, then sonicated in ethanol for 10 min and finally dried with a flow of nitrogen gas.

2.2. Preparation of 2-MT SAM on Copper

The pre-treated electrodes were instantly assembled in different concentrations of 2-MT solution for different assembly time at room temperature. Finally, the assembled copper electrode was taken out from the 2-MT solutions and rinsed with anhydrous ethanol solution followed by double distilled water to remove physisorbed 2-MT molecules on the electrode surface and then dried by flowing nitrogen gas prior to their use for further examinations.

2.3. Electrochemical Methods

Electrochemical analysis tests were carried out at room temperature in a conventional three-electrode cell system with a saturated calomel electrode (SCE), counter electrode and copper electrode with exposed surface area of 1 cm^2 as reference, auxiliary and working electrodes, respectively. The electrochemical measurements were performed on CHI electrochemical workstation (CHI 760D). During the electrochemical studies, the working electrodes were kept in the 3% NaCl solution for 1 h to stabilize the open-circuit potential (OCP). The electrochemical impedance spectroscopy (EIS) measurements were carried out under OCP sweep frequency from 100000 Hz to 0.1 Hz with amplitude of 5 mV. The obtained EIS results were analyzed by ZSimpWin 3.2.1 software and fitted to the appropriate electrical equivalent circuits. The potentiodynamic polarization curves were obtained from -250 to $+250$ mV with a scan rate of 2 mV s^{-1} in 3% NaCl solution.

2.4. Surface Characterization

Fourier transform infrared (FT-IR) spectra were taken using JASCO 460 plus model spectrometer and were scanned in the wavenumber range of 400 to 4000 cm^{-1} with a resolution of 4 cm^{-1} . Scanning electron microscopy (SEM) and elemental analysis of the copper substrates were performed on SEM-EDX instrument (VEGA3 TESCAN, and EDX, Bruker Nano, Germany). The contact

angle on the bare copper and 2-MT modified copper were measured on a contact angle goniometer (CA, 250-F1, rame-hart instrument Co., USA) by a sessile droplet method. The surface roughness of the copper with and without SAM surfaces was measured by using an atomic force microscope (AFM, BT 02218, Nanosurf, Switzerland) operating in contact mode recorded at scanning area of $10 \times 10 \mu\text{m}$ with a scan speed of 10 mm s^{-1} .

3. RESULTS AND DISCUSSION

3.1. Electrochemical Impedance Spectroscopy

3.1.1. Effect of Concentration

Figure 2 illustrates the Nyquist and Bode plots in 3% NaCl solution for the bare electrode and 2-MT covered electrodes, which were assembled in different concentration of 2-MT in ethanol at an assembly time of 12 h. Nyquist plot of bare electrode is composed of two parts:

- (i) the depressed semicircle in the high frequency accredited to the frequency dispersion because of the inhomogeneous and roughness of the electrode surface.²⁵ and
- (ii) Warburg impedance at low frequency represents the transportation of oxygen from the bulk solution to the surface of the copper substrate.^{26–28}

Considering that the impedance of a C_{dl} does not perform as a pure capacitor in the presence of frequency dispersion, herein constant phase element (CPE) was employed as an alternative of C_{dl} in the equivalent circuit models and can more correctly fit the experimental EIS data.²⁹ The impedance of a CPE is defined as follows,

$$Z_{CPE} = \frac{1}{Y_0(j\omega)^{-n}} \quad (1)$$

where Y_0 is the magnitude of the CPE, j represents the imaginary root, ω is the angular frequency and n is the phase which can be related to state of electrode surface. The EIS parameters obtained by fitting the impedance plots with different electrochemical equivalent circuit models are shown in Figure 2(a) (inset). The parameters of the equivalent circuit comprise namely, R_s , R_{ct} , R_{sam} , W , CPE_{dl} and CPE_{sam} . Where, R_s stands for the electrolytic solution resistance, R_{ct} is the charge transfer resistance, R_{sam} is the resistance of 2-MT SAM, W is the Warburg impedance and CPE_{dl} and CPE_{sam} are representing the constant phase element of electrical double layer and constant phase element of SAM, respectively and are listed in Table I. Figures 2(b) and (c) shows the Bode plots (phase angle vs. frequency and impedance vs. frequency) of bare electrode and 2-MT SAM covered copper electrodes in 3% NaCl solution. By the comparison with the bare electrode, the 2-MT covered electrode showed a wider domain and higher negative phase angle value at the high frequency which was increased by increasing the SAM concentration (Fig. 2(b)). This indicates the more compact and stable protective barrier layer on the electrode surface.

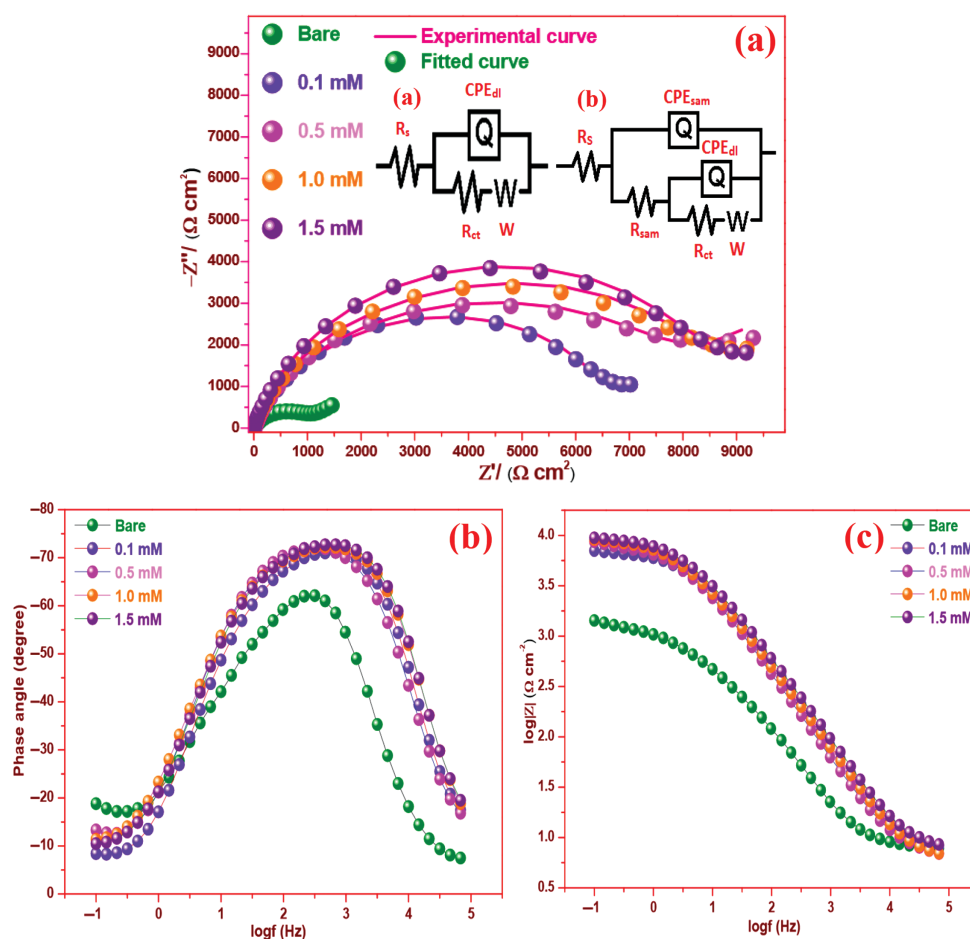


Figure 2. (a) Nyquist and (b and c) Bode plots obtained in 3% NaCl for bare copper and 2-MT covered copper electrodes assembled in different concentrations of 2-MT solution for 12 h. (inset (a): Equivalent circuits used for fitting impedance spectra of bare and 2-MT covered copper).

On the other hand, Bode curve shows highest impedance modulus at low frequency which is noticed with increasing SAM concentration (Fig. 2(c)), revealing the higher surface coverage on the electrode surface.

An increase in the concentration of 2-MT increases the R_{ct} values and decreases the CPE values (Table I). The increase in R_{ct} value implies that the formation of 2-MT SAM on copper by adsorption of 2-MT molecules which impedes the diffusion of corrosive species from corrosive solution to the underlying electrode surface and

Table I. Nyquist impedance parameters for the bare copper and copper electrodes assembled in different concentrations of 2-MT solution for 12 h in 3% NaCl solution.

C (mM)	R_{ct} ($\Omega \text{ cm}^2$)	CPE_{dl} ($\mu\text{F cm}^{-2}$)	n_1	R_{sam} ($\Omega \text{ cm}^2$)	CPE_{sam} ($\mu\text{F cm}^{-2}$)	n_2	IE (%)
0	995	59.84	0.75	–	–	–	–
0.1	4288	10.58	0.73	2388	6.70	0.80	76.79
0.5	6542	9.56	0.80	2401	3.23	0.84	84.79
1.0	8694	9.02	0.82	4219	12.80	0.87	88.55
1.5	8732	7.71	0.80	6169	10.79	0.76	88.60

thus reduces the speed of the corrosion reactions. The CPE value of the 2-MT covered electrodes decreased significantly than that of the bare electrode. Moreover, the decrease in CPE values were observed while increasing the concentration of 2-MT, this can be attributed to the adsorption of 2-MT molecules on surface of the electrode resulting in decline in local dielectric constant or growth in the double layer of the thickness.³⁰ The increase in n values infers a reduction of the surface inhomogeneity owing to the formation of compact and ordered monolayer on the electrode surface.³¹ For the copper electrode assembled in 0.1 mM 2-MT solution, the R_{ct} is 4288 $\Omega \text{ cm}^2$. With an increase in assembling concentration of 2-MT from 0.5 to 1.0 mM, R_{ct} values increased from 6542 to 8694 $\Omega \text{ cm}^2$. In addition, the value of inhibition efficiency increased by increasing the SAM concentrations with maximal value reaches of 88.55% at 1.0 mM 2-MT. Further, when the concentration of SAM rises to 1.5, there is a slight increase for inhibition efficiency. Therefore, 1.0 mM of 2-MT was selected as optimum concentration to prepare the SAM on the copper surface.

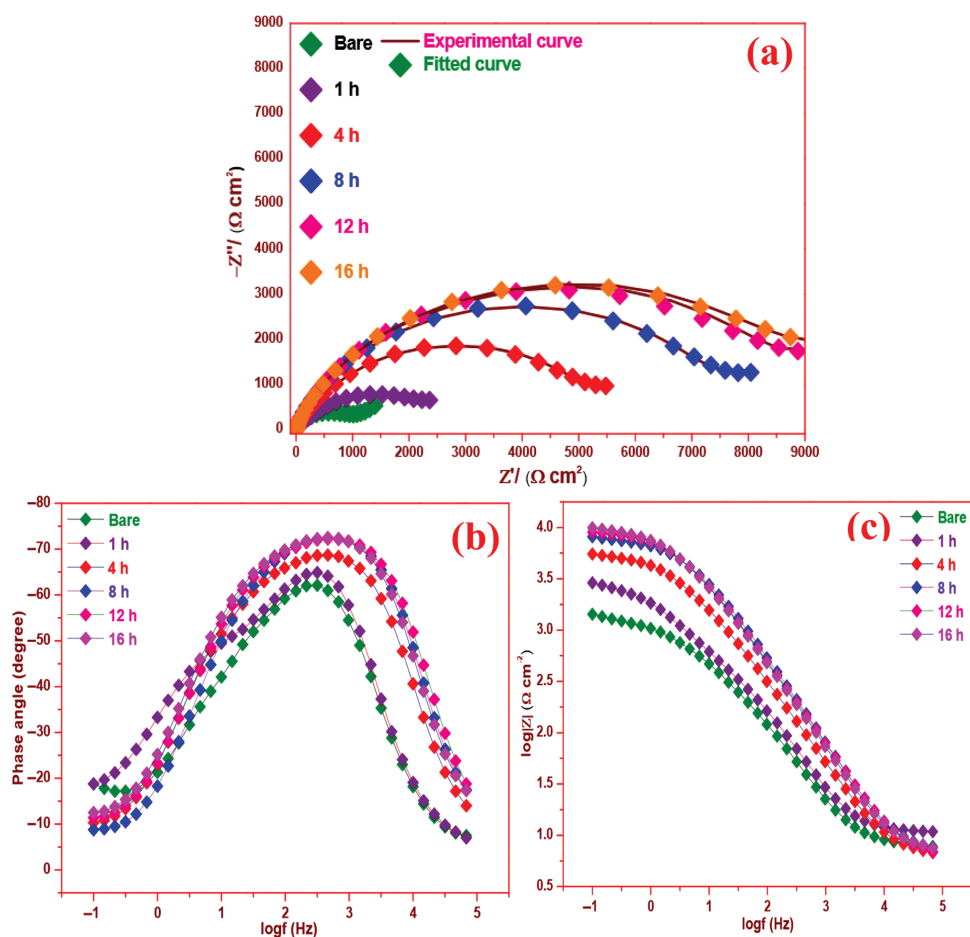


Figure 3. (a) Nyquist plot and Bode plots (b and c) obtained in 3% NaCl for bare copper and 2-MT covered copper electrodes assembled in 1.0 mM 2-MT solution for different time.

3.1.2. Effect of Assembly Time

The optimal concentration of 1.0 mM 2-MT was assembled on copper at different assembly times (1–16 h). Electrochemical impedance spectra in the form of Nyquist and Bode plots for bare copper and 2-MT covered copper electrodes were recorded in 3% NaCl solution (Fig. 3) and the corresponding impedance parameters are given in Table II. As shown in Table II that R_{ct} value of bare electrode is very low ($995 \Omega \text{ cm}^2$). When the electrode is assembled with 2-MT (1.0 mM) for 1 h, the R_{ct} value

increases to $2005 \Omega \text{ cm}^2$, indicating the formation of 2-MT SAM on electrode surfaces is a fast adsorption process. On increasing the assembling time to 4 h, there is a slight increase in the R_{ct} from 2005 to $3518 \Omega \text{ cm}^2$. Moreover,

Table II. Nyquist impedance parameters for the bare copper and copper electrodes assembled in 1.0 mM 2-MT solution for different time in 3% NaCl solution.

t (h)	R_{ct} ($\Omega \text{ cm}^2$)	CPE_{dl} ($\mu\text{F cm}^{-2}$)	n_1	R_{sam} ($\Omega \text{ cm}^2$)	CPE_{sam} ($\mu\text{F cm}^{-2}$)	n_2	IE (%)
0	995	59.84	0.75	–	–	–	–
1	2005	22.66	0.68	1043	10.47	0.82	50.37
4	3518	20.19	0.71	1722	13.44	0.84	71.71
8	4775	13.06	0.73	2810	6.45	0.78	79.16
12	8694	12.80	0.82	4219	9.02	0.87	88.55
16	9148	13.29	0.81	4729	2.55	0.77	89.12

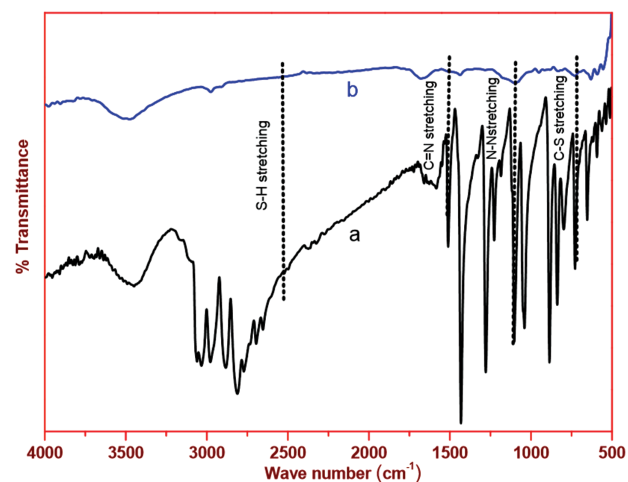


Figure 4. FT-IR spectra of (a) solid 2-MT and (b) 2-MT SAM covered copper.

R_{ct} values sharply increased by prolonging assembly times from 8 to 12 h (4775 to 8694 $\Omega \text{ cm}^2$). This result indicates that formation of well-ordered packed monolayer on the electrode surface at 12 h. Moreover, the inhibition efficiency increased when increasing the time. A maximal value for inhibition efficiency of 88.55% was found at 12 h and further increase in assembly time to 16 h does not exhibit significant increase in inhibition efficiency (89.12%). These results represent that the SAM molecules on copper have reached an ordered SAM at 12 h assembling time. In addition to that, the CPE values decreases (59.84 to 12.80 $\mu\text{F cm}^{-2}$) and the n values increase (0.75 to 0.82) by increasing assembly time of 12 h. Thus, the best immersion time is found to be 12 h for the 2-MT SAM formation. The optimal concentration of 1.0 mM 2-MT with the 12 h assembling time is employed for the development of 2-MT SAM on copper surface throughout this study.

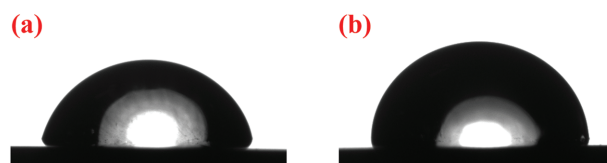


Figure 6. Contact angle images of (a) polished copper and (b) 2-MT SAM covered copper.

3.2. Characterization of Surface Film

3.2.1. Morphological Analysis

FT-IR analysis of the solid 2-MT and 2-MT covered copper were performed to detect the nature of the present functional groups at the copper surface.^{32,33} The IR spectrum of solid 2-MT (Fig. 4(a)) displays characteristic absorption bands at 1511, 1103, 729 and 2552 cm^{-1} corresponding to C=N, N-N, C-S, and S-H stretching,

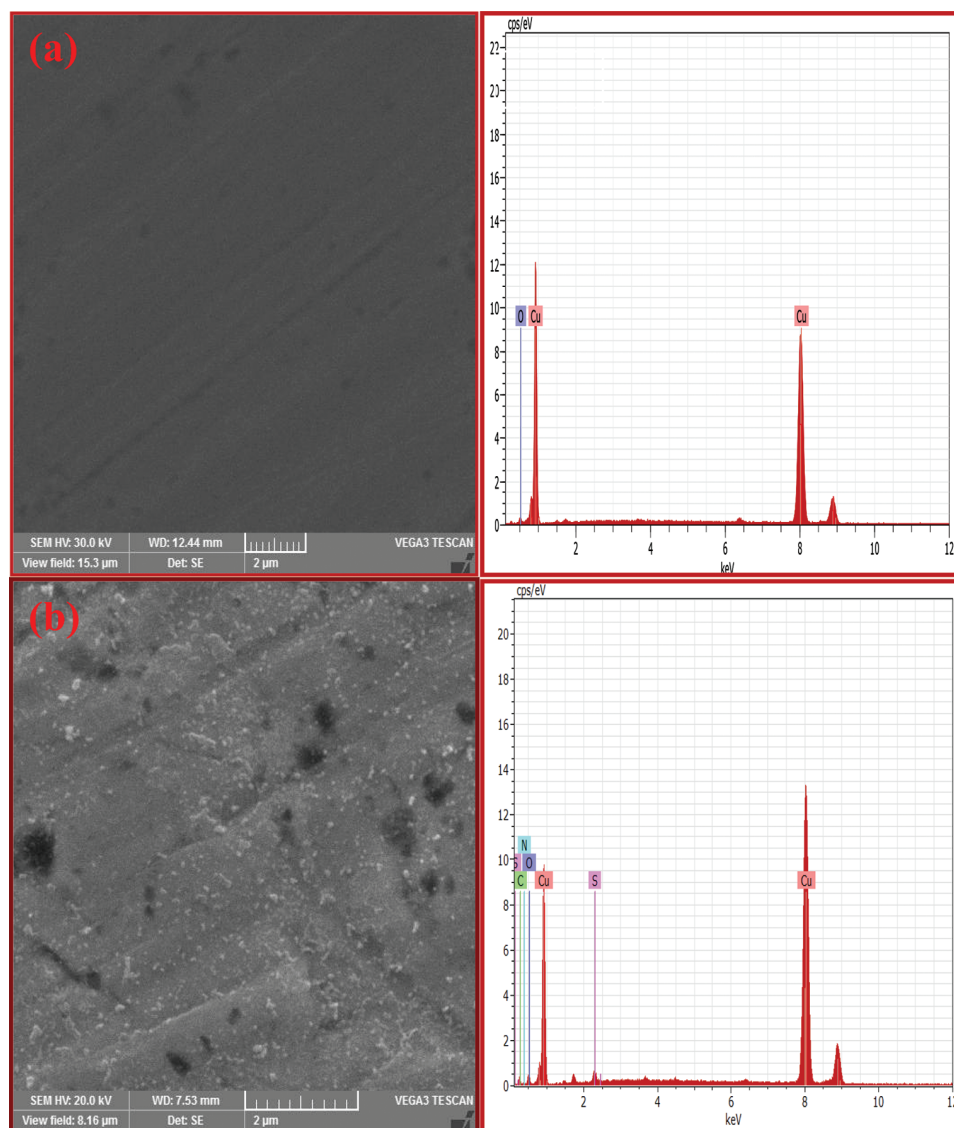


Figure 5. SEM images and EDX spectra of (a) polished copper and (b) 2-MT SAM covered copper.

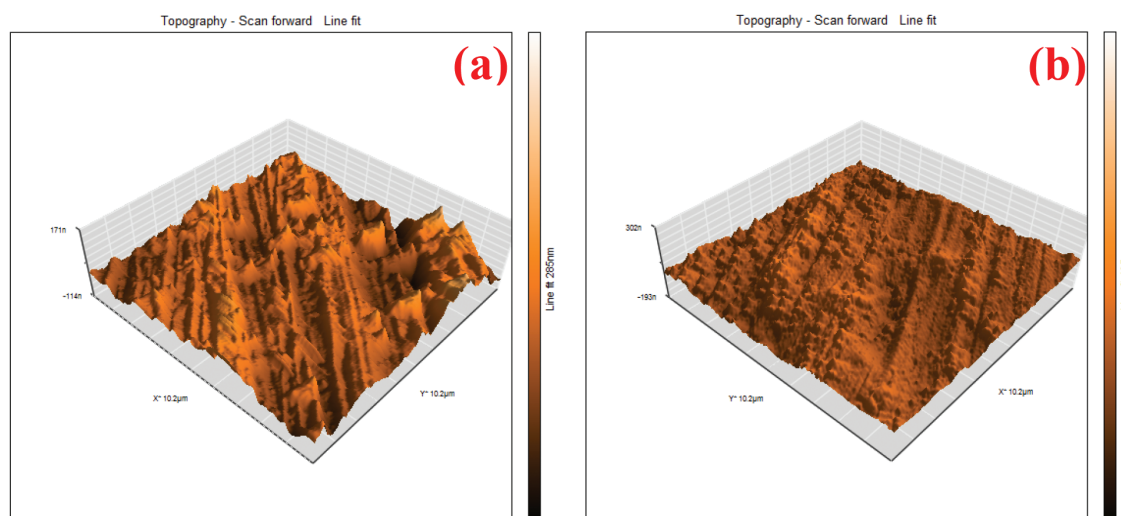


Figure 7. AFM images of (a) polished copper and (b) 2-MT SAM covered copper.

respectively.³⁴ By comparing the solid 2-MT, the spectrum of 2-MT covered copper shifted the absorption bands to the lower frequencies (Fig. 4(b)). The absence of S–H stretching band at 2552 cm^{-1} confirms the formation Cu–S bond at the copper surface after cleavage of S–H bond. The bands at 1462 and 1030 cm^{-1} are corresponding to C=N and N–N stretching, respectively and these band showed an appreciable shift in position of the C=N, N–N for the 2-MT SAM covered copper compared with the solid 2-MT. These results might point out that the 2-MT molecules were adsorbed on copper by the N and S atoms in 2-MT molecule.

The successful modification of 2-MT on copper was well supported by SEM and EDX analyses. The polished copper (Fig. 5(a)) represents the few notches and polishing scratches on surface due to pretreatment process by emery papers. The EDX spectrum of bare Cu displays

two peaks belonging to O (0.53 keV) and Cu (0.93 and 8.05 keV), respectively. On the other hand, after modification with 2-MT (Fig. 5(b)), the morphology of surface seems uniform which could be due to SAM formation. Correspondingly, the EDX spectrum exhibits four peaks accountable to C (0.28 keV), N (0.39 keV), S (2.15 keV) and O (0.53 keV) confirming that the 2-MT molecules are successfully prepared on the copper surface.

3.2.2. Contact Angle

Contact angle analysis was used to examine the surface wettability of bare copper and 2-MT SAM formed on copper surface. The bare copper surface (Fig. 6(a)) shows smooth morphology with a CA of 77.5° . After surface modification with 2-MT (Fig. 6(b)), the CA of the copper is 87.6° , an increase to that of the bare copper, and it might be accredited to the formation of the 2-MT SAM on the copper substrate.

3.2.3. Atomic Force Microscopy

The surface roughness and topography of the copper in the absence and the presence of 2-MT SAM was examined by AFM. The AFM patterns of 3D-topography for the polished and 2-MT modified copper sample are shown in Figure 7. Figure 7(a) shows smooth morphology with some polished scratches with the average surface

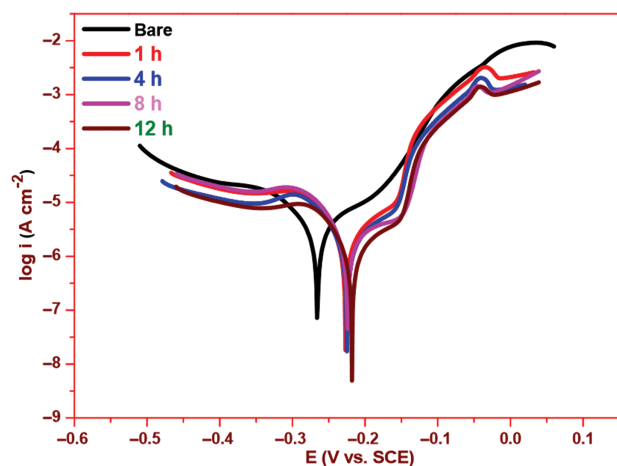


Figure 8. Polarization curves obtained in 3% NaCl solution for bare copper and 2-MT covered copper electrodes assembled in 1.0 mM 2-MT solution for different time.

Table III. Polarization parameters for bare copper and copper electrodes assembled in 1.0 mM 2-MT solution for different time in 3% NaCl solution.

t (h)	$-E_{\text{corr}}$ (mV/SC)	I_{corr} ($\mu\text{A cm}^{-2}$)	IE (%)
0	266	5.464	–
1	227	1.922	64.82
4	225	1.651	69.78
8	224	1.539	71.83
12	217	1.500	72.54

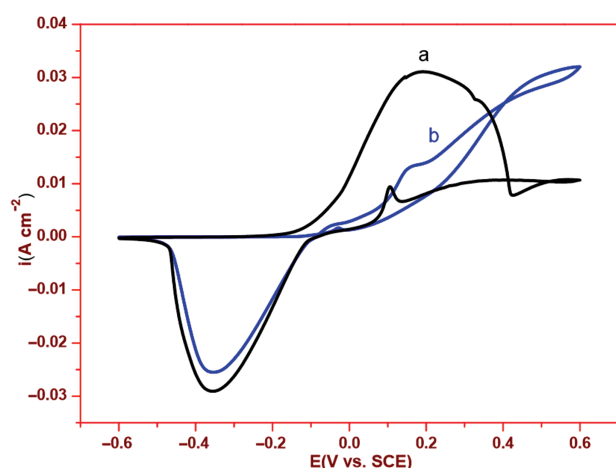


Figure 9. Cyclic voltammograms of (a) bare copper and (b) 2-MT SAM covered copper electrodes in 3% NaCl solution.

roughness (S_a) and the root mean square (S_q) of copper was measured to be 19.766 and 24.965 nm. Whereas, in presence of SAM (Fig. 7(b)) the S_a and S_q are 16.844 and 20.834 nm, respectively and this decrease has demonstrated that the 2-MT molecules were chemically adsorbed on the copper surface and decreased the roughness of the copper substrate surface.

3.3. Corrosion Protection of Copper by 2-MT SAM

3.3.1. Potentiodynamic Polarization Studies

Figure 8 depicts potentiodynamic polarization plots for copper in 3% NaCl solution in the absence and presence of 2-MT SAM formed at different assembly time. The electrochemical polarization parameters for copper electrodes were determined from Tafel extrapolation method³⁵ and corresponding parameters were recorded in Table III.

The inhibition efficiency can be determined as follows.³⁶

$$IE (\%) = \frac{i_{\text{corr}}^0 - i_{\text{corr}}}{i_{\text{corr}}^0} \times 100 \quad (2)$$

Where i_{corr}^0 and i_{corr} are the corrosion currents in the absence and the presence of 2-MT SAM modified copper, respectively. From Figure 8, it is clear that the presence of SAM significantly suppresses both anodic and cathodic polarization curves and shifts the corrosion potential (E_{corr}) to anodic direction than that of the bare electrode. The decrease of anodic and cathodic curves with increasing assembly time is due to the formation of thicker protective SAM on the electrode surface by the adsorption of 2-MT molecules. Further, the corrosion current (i_{corr}) values were sharply decreased in the presence of 2-MT. As can be found in Table III, the bare electrode i_{corr} is $5.464 \mu\text{A cm}^{-2}$, for the copper covered with 2-MT SAM of different assembly time viz., 1, 4, 8 and 12 h, the i_{corr} decreased to 1.922, 1.651, 1.539 and $1.500 \mu\text{A cm}^{-2}$, respectively. The observed decrease in i_{corr} showed that the electrode surface had a harder tendency to copper dissolution after the adsorption of the SAM. Inhibition efficiency values increases from 64.82 to 72.54%. It is observed that, the E_{corr} of the copper shifted anodically (positive) from -266 to -217 mV after covered with 2-MT SAM, which corroborated the anticorrosive ability of 2-MT monolayer on the electrode surface. In the present study, the maximum shift in E_{corr} in the absence and presence of the SAM, were lower than 85 mV.³⁷ As a result, the 2-MT compound was defined as mixed type inhibitor with predominantly inhibiting the anodic process than cathodic process.

3.3.2. Cyclic Voltammetric Studies

Cyclic voltammetric studies were carried out to elucidate the protective surface film formed on the copper surface.

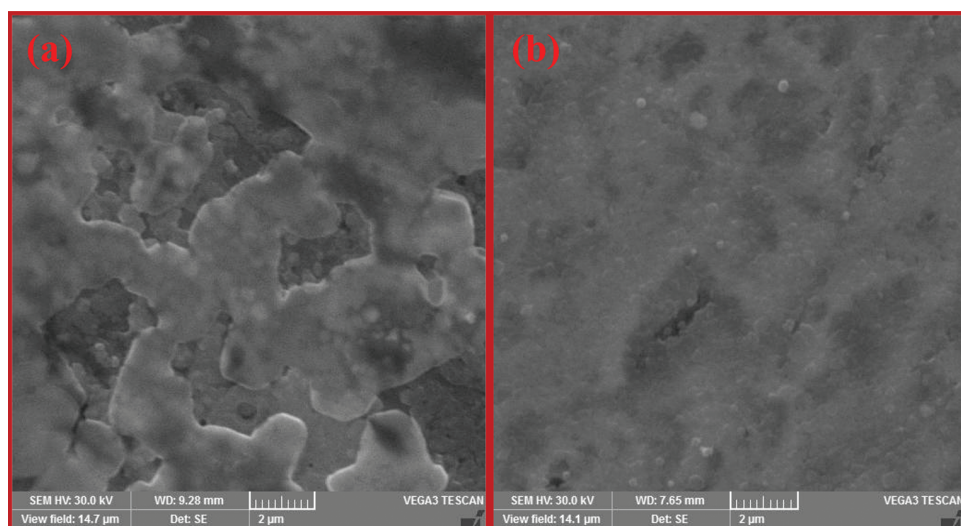
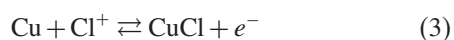


Figure 10. SEM images of (a) bare copper and (b) 2-MT SAM covered copper after 3 days immersion in 3% NaCl solution.

The cyclic voltammogram recorded for copper electrode with and without SAM are shown in Figure 9. It can be seen from Figure 9(a) that the bare copper exhibits two oxidation peaks at the forward cycle at 0.19 and 0.35 V (SCE), respectively. The first peak is attributed to the oxidation of Cu(0) to the CuCl salt layer and the second peak is the further oxidation of CuCl to the soluble CuCl_2^- species as described by reaction (3) and (4), respectively.^{38–40} Correspondingly, there is a single large reduction peak arising at -0.36 V (SCE) which can be attributed to the corrosion product of CuCl can be partially reduced to Cu(0) state Eq. (5).



Compared with the bare Cu, the CV curve showed that peak domain and peak height for copper covered with 2-MT greatly suppressed in the forward scan while the reduction peak height decreases evidently in the reverse scan (Fig. 9(b)). These observations exhibit that 2-MT molecules are assembled on the copper electrode and the oxidation and reduction reactions of copper, especially from Cu(0) to Cu(I), are blocked evidently. These results confirm the 2-MT SAM on copper has good anticorrosion protection for the bare copper substrate.

3.3.3. Scanning Electron Microscopy

In order to further confirm the corrosion resistance capability of the 2-MT SAM on copper, SEM was recorded to study the surface morphology of the bare copper and 2-MT covered copper after immersion in 3% NaCl solution for 3 days. Figure 10(a) portrays the surface of copper is highly damaged due to the metal dissolution in the corrosive solution while 2-MT SAM covered copper surface (Fig. 10(b)) exhibit smooth and less rusted morphology compared with the bare copper. It can be suggested that the 2-MT SAM on surface can effectively prevent diffusion of corrosive particle ions onto the copper surface.

4. CONCLUSION

In this paper, we focused the development of 2-mercapto-1,3,4-thiadiazole monolayer on copper surface by a self-assembly system and its characterization by FT-IR, SEM, EDX, contact angle and AFM analysis. The FT-IR and EDX results corroborated the formation of the 2-MT on the copper surface and also showed that the 2-MT molecule was chemically adsorbed on the copper surface by the nitrogen and sulphur atoms. Corrosion resistance properties of 2-MT copper were evaluated by PDS, CV and SEM analysis. Polarization plots show that 2-MT acts as mixed inhibitor, primarily in anodic nature and with maximum protection efficiency of 72.54%.

Acknowledgments: P. Durainatarajan is grateful to the UGC-RFSMS (Research Fellowship in Sciences for Meritorious Students, Grant No: F.No.25-1/2014-15/(BSR)/7-225/2008/(BSR), dt: 7th October 2015) for financial support and also the authorities of The Gandhigram Rural Institute for encouragement.

References and Notes

1. L. Nunez, E. Reguera, F. Corvo, E. Gonzalez, and C. Vazquez, *Corros. Sci.* 47, 461 (2005).
2. A. Shaban, E. kálmán, and J. Telegdi, *Electrochim. Acta* 43, 159 (1998).
3. C. Liang, P. Wang, B. Wu, and N. Huang, *J. Solid State Electrochem.* 14, 1391 (2010).
4. G. Kear, B. Barker, and F. Walsh, *Corros. Sci.* 46, 109 (2004).
5. D. Wang, B. Xiang, Y. Liang, S. Song, and C. Liu, *Corros. Sci.* 85, 77 (2014).
6. A. Ulman, *Chem. Rev.* 96, 1533 (1996).
7. J. C. Love, L. A. Estroff, J. K. Kriebel, R. G. Nuzzo, and G. M. Whitesides, *Chem. Rev.* 105, 1103 (2005).
8. C. M. Ruan, T. Bayer, S. Meth, and C. N. Sukenik, *Thin Solid Films* 419, 95 (2002).
9. J. D. Talati and D. K. Gandhi, *Corros. Sci.* 23, 1315 (1983).
10. M. Yadav and D. Sharma, *Indian J. Chem. Technol.* 17, 95 (2010).
11. E. M. Sherif, *Appl. Surf. Sci.* 252, 8615 (2006).
12. K. Es-Salah, M. Keddad, K. Rahmouni, A. Srhiri, and H. Takenouti, *Electrochimica. Acta* 49, 2771 (2004).
13. M. M. Antonijevic, S. M. Milic, and M. B. Petrovic, *Corros. Sci.* 51, 1228 (2009).
14. W. Chen, H. Q. Luo, and N. B. Li, *Corros. Sci.* 53, 3356 (2011).
15. Y. C. Pan, Y. Wen, R. Zhang, Y. Y. Wang, Z. R. Zhang, and H. F. Yang, *Appl. Surf. Sci.* 258, 3956 (2012).
16. Y. C. Pan, Y. Wen, X. Y. Guo, P. Song, S. Shen, Y. P. Du, and H. F. Yang, *Corros. Sci.* 73, 274 (2013).
17. Y. Qiang, S. Zhang, S. Xu, and L. Yin, *RSC Adv.* 5, 63866 (2015).
18. T. N. J. I. Edison and M. G. Sethuraman, *ISRN Electrochem.* 2013, 1 (2013).
19. H. Tian, W. Li, K. Cao, and B. Hou, *Corros. Sci.* 73, 281 (2013).
20. S. Varvara, L. M. Muresan, K. Rahmouni, and H. Takenouti, *Corros. Sci.* 50, 2596 (2008).
21. E. M. Sherif and S. M. Park, *Corros. Sci.* 48, 4065 (2006).
22. B. V. Appa Rao, Md. Yakub Iqbal, and B. Sreedhar, *Corros. Sci.* 51, 1452 (2009).
23. W. Chen, S. Hong, H. B. Li, H. Q. Luo, M. Li, and N. B. Li, *Corros. Sci.* 61, 53 (2012).
24. T. T. Qin, J. Li, H. Q. Luo, M. Li, and N. B. Li, *Corros. Sci.* 53, 1072 (2011).
25. X. Wu, H. Ma, S. Chen, Z. Xu, and A. Sui, *J. Electrochem. Soc.* 146, 1847 (1999).
26. Y. Feng, K. S. Siow, W. K. Teo, K. L. Tan, and A. K. Hsieh, *Corrosion* 53, 389 (1997).
27. H. Y. Ma, C. Yang, S. H. Chen, Y. L. Jiao, S. X. Huang, D. G. Li, and J. L. Luo, *Electrochim. Acta* 48, 4277 (2003).
28. N. Karthik, T. N. J. I. Edison, Y. R. Lee, and M. G. Sethuraman, *Taiwan Inst. Chem. Eng.* 77, 302 (2017).
29. G. Y. Li, H. Y. Ma, Y. L. Jiao, and S. H. Chen, *J. Serb. Chem. Soc.* 69, 791 (2004).
30. X. H. Zhang, Q. Q. Liao, K. B. Nie, L. L. Zhao, D. Yang, Z. W. Yue, H. H. Ge, and Y. J. Li, *Corros. Sci.* 93, 201 (2015).
31. F. B. Growcock and R. J. Jasinski, *J. Electrochem. Soc.* 136, 2310 (1989).
32. T. N. J. I. Edison, R. Atchudan, N. Karthik, and Y. R. Lee, *Int. J. Hydrogen Energy*, 42, 14390 (2017).

33. T. N. J. I. Edison, R. Atchudan, M. G. Sethuraman, and Y. R. Lee, *Taiwan Inst. Chem. Eng.* 68, 489 (2016).
34. A. Lalitha, S. Ramesh, and S. Rajeswari, *Electrochim. Acta* 51, 47 (2005).
35. T. N. J. I. Edison, R. Atchudan, N. Karthik, M. G. Sethuraman, and Y. R. Lee, *Taiwan Inst. Chem. Eng.* 80, 901 (2017).
36. P. Wang, C. Liang, B. Wu, N. Huang, and J. Li, *Electrochimica. Acta* 55, 878 (2010).
37. W. H. Li, Q. He, S. T. Zhang, C. L. Pei, and B. R. Hou, *J. Appl. Electrochem.* 38, 289 (2008).
38. D. G. Li, S. H. Chen, S. Y. Zhao, and H. Y. Ma, *Colloids Surf. A* 273, 16 (2006).
39. Q. Q. Liao, Z. W. Yue, D. Yang, Z. H. Wang, Z. H. Li, H. H. Ge, and Y. J. Li, *Corros. Sci.* 53, 1999 (2011).
40. Y. M. Lee, Y. H. C. Chien, M. K. Leung, C. C. Hu, and C. C. Wan, *J. Mater. Chem. A* 1, 3629 (2013).

Received: 1 September 2017. Accepted: 30 October 2017.

IP: 212.12.213.32 On: Sun, 17 Jun 2018 18:27:20
Copyright: American Scientific Publishers
Delivered by Ingenta